Rearrangement of Protonated Propene Oxide to Protonated Propanal

James M. Coxon,*,† Robert G. A. R. Maclagan,† Arvi Rauk,‡ Aaron J. Thorpe,† and Dale Whalen§

Contribution from the Departments of Chemistry, University of Canterbury, Christchurch, New Zealand, University of Maryland Baltimore County, Baltimore, Maryland 21228-5398, and University of Calgary, Alberta, Canada T2N 1N4

Received August 30, 1996[⊗]

Abstract: Calculations at the MP2/6-31G*//MP2/6-31G* level show there are concerted asynchronous pathways connecting protonated propene oxide and protonated propanal. With cleavage of the C−O bond of protonated propene oxide, the preference for rotation of oxygen away from the more hindered face of the oxirane plane containing the methyl group is quantified as 2 kcal/mol. This pathway involves two distinct steps; first, rupture of the oxirane and, second, hydride migration. The latter does not commence until rupture of the C−O bond is complete. The combination of these two steps defines a concerted asynchronous rearrangement pathway. The reaction is predicted to show a 20:1 preference for migration of the proton *trans* to the methyl over the *cis*.

Introduction

The rearrangement of oxiranes to carbonyl compounds, like nucleophilic substitution at a saturated carbon, is representative of a reaction of fundamental importance in organic synthesis. Rearrangement can be catalyzed by proton or Lewis acid,[1] inducing a hydrogen, alkyl, or aryl atom to migrate between adjacent carbons in the carbonyl-forming step. Many arene oxides react in aqueous solution by both spontaneous and acid-catalyzed pathways to give diols and phenols.[2] In this latter reaction the 1,2-hydride migration leading to an intermediate cyclohexadienone is referred to as an "NIH shift."[3] This occurs in nature, for example, in the biosynthesis of tyrosine.[4] Oxiranes sufficiently activated by substituent aryl and vinyl groups also yield carbonyl products in aqueous solution by the spontaneous reaction pathway.

Acid-induced rearrangement of epoxides by alkyl, aryl, or hydrogen migration was for many years considered to be a concerted process. However, for epimeric pairs of exocyclic tertiary substituted epoxides, acid-catalyzed rearrangement results in similar mixtures of epimeric aldehydes[5] consistent with a stepwise rearrangement involving the intermediacy of carbocations (Figure 1).

For each epimeric epoxide, where conformation is defined, for example, by a 4-*tert*-butyl group or by fusion to a second ring, a marginal preference for the aldehyde resulting from inversion is observed, *i.e.* **4** from **1** and **8** from **5**. The formation, however, of aldehyde **4** along with **8** from **5** is evidence for the intermediacy of a carbocation. A concerted hydride migration from **5** would give only **8**. The fact that **4** is also formed is consistent with the reaction proceeding at least in part via a carbocation. On cleavage of the more substituted C−O bond, rotation about the C^+-CH_2O bond in either direction places a hydrogen *anti* to the original C−O in a geometry favorable for hydrogen migration. This necessarily occurs before further rotation places a hydrogen *syn* to the original C−O bond. For example epoxide **5** opens to **6** and rotation to **7** (or the mirror image) occurs before formation of **3** (or the mirror image). Provided that the rate of bond rotation converting **7** to **3** is not rapid relative to hydride migration a preference for formation of **8** from **5** will be observed. By the same argument, reaction of **1** would be expected to give a higher yield of **4** than **8**. The extent of bias for the product of inversion at C2 contains information about the relative rate of rotation and hydride migration. For example, if rotation is fast relative to hydride migration then both epimeric epoxides should give an identical ratio of epimeric aldehydes, which is not observed.[6]

[⊗] Abstract published in *Advance ACS Abstracts,* May 1, 1997.

(1) Norman, R. O. C.; Coxon, J. M. *Principles of Organic Synthesis,* 3rd ed.; Blackie, Chapman and Hall: London, 1993; p 590.

(2) Ross, A. M.; Pohl, T. M.; Piazza, K.; Thomas, M.; Fox, B.; Whalen, D. L. *J. Am. Chem. Soc.* **1982**, *104*, 1658. Gillilan, R. E.; Pohl, T. M.; Whalen, D. L. *J. Am. Chem. Soc.* **1982**, *104*, 4481−4482. Gupta, S. C.; Pohl, T. M.; Friedman, S. L.; Whalen, D. L.; Jerina, D. M. *J. Am. Chem. Soc.* **1982**, *104*, 3101. Sayer, J. M.; Yagi, H.; Silverton, J. V.; Friedman, S. L.; Whalen, D. L.; Jerina, D. M. *J. Am. Chem. Soc.* **1982**, *104*, 1972. Sayer, J. M.; Whalen, D. L.; Friedman, S.; Paik, S.; Yagi, H.; Vyas, K. D.; Jerina, D. M. *J. Am. Chem. Soc.* **1984**, *106*, 226. Ukachukwu, V. C.; Blumenstein, J. J.; Whalen, D. L. *J. Am. Chem. Soc.* **1986**, *108*, 5039. Islam, N. B.; Whalen, D. L.; Yagi, H.; Jerina, D. M. *J. Am. Chem. Soc.* **1987**, *109*, 2108. Gupta, S. C.; Islam, N. B.; Whalen, D. L.; Yagi, H.; Jerina, D. M. *J. Org. Chem.* **1987**, *52*, 3812. Ukachukwu, V. C.; Whalen, D. L. *Tetrahedron Lett.* **1988**, *29*, 293. Islam, N. B.; Whalen, D. L.; Yagi, H.; Jerina, D. M. *Chem. Res. Toxicol.* **1989**, *1*, 398. Islam, N. B.; Gupta, S. C.; Yagi, H.; Jerina, D. M.; Whalen, D. L. *J. Am. Chem. Soc.* **1990**, *112*, 6363. Nashaat, N. T.; Balani, S. K.; Loncharich, R. J.; Shipley, D. Y.; Mohan, R. S.; Whalen, D. L.; Jerina, D. M. *J. Am. Chem. Soc.* **1991**, *113*, 3910.

(3) Jerina, D.; Daly, J.; Witkop, B.; Zaltaman-Nirenberg, P.; Underfriend, S. *Arch. Biochem. Biophys.* **1969**, *128*, 176. Jerina, D. M.; Daly, J. W.; Witkop, B.; Zaltaman-Nirenberg, P.; Underfriend, S. *Biochemistry* **1970**, *9*, 147. Jerina, D. M.; Daly, J. W.; Witkop, B.; Zaltaman-Nirenberg, P.; Underfriend, S. *J. Am. Chem. Soc.* **1968**, *90*, 6523−6525. Boyd, D. R.; Jerina, D. M.; Daly, J. *J. Org. Chem.* **1970**, *35*, 3170. Boyland, E.; Sims, P. *Biochem. J.* **1965**, *95*, 788.

(4) Dipple, A.; Moschel, R. C.; Bigger, A. H. *Chemical Carcinogens,* 2nd ed.; Searle, C. E., Ed.; ACS Monograph 182; American Chemical Society: Washington, DC, 1984; Vol. 1, p 41. *Polycyclic. Hydrocarbons. and Carcinogenesis,* Harvey, R. G., Ed.; ACS Symposium Series 283, American Chemical Society: Wshington, DC, 1985. *Polycyclic, Hydrocarbons, and Cancer*; Gelboin, H. V., Tso, P. O. P., Eds.; Academic Press: New York, 1978; Vol. 1.

(5) Blackett, B. N.; Coxon, J. M.;Hartshorn, M. P.; Jackson, B. L. J .; Muir, C. N. *Tetrahedron* **1969**, *25*, 1479.

(6) Blackett, B. N.; Coxon, J. M.; Hartshorn, M. P.; Richards. K. E. *Aust. J. Chem.* **1970**, *23*, 839. Blackett, B. N.; Coxon, J. M.; Hartshorn, M. P.; Richards, K. E. *J. Am. Chem. Soc.* **1970**, *92*, 2574. Blackett, B. N.; Coxon, J. M.; Hartshorn, M. P.; Richards, K. E. *Aust. J. Chem.* **1970**, *23*, 2077. Coxon, J. M.; Lim, C.-E. *Aust. J. Chem.* **1977**, *30*, 1137. Coxon, J. M.; McDonald, D. Q. *Tetrahedron Lett.* **1988**, *29*, 2575.

S0002-7863(96)03057-0 CCC: $14.00

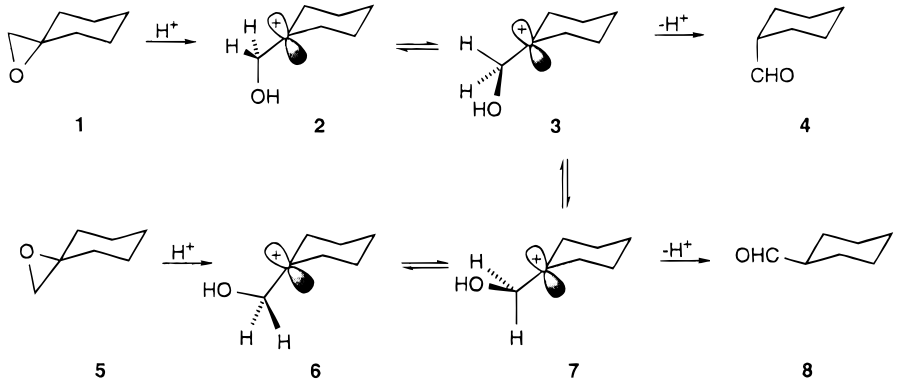

Figure 1. Schematic representation of epoxide rearrangement. (Configuration defined *e.g.* by a 4-*tert*-Bu group.)

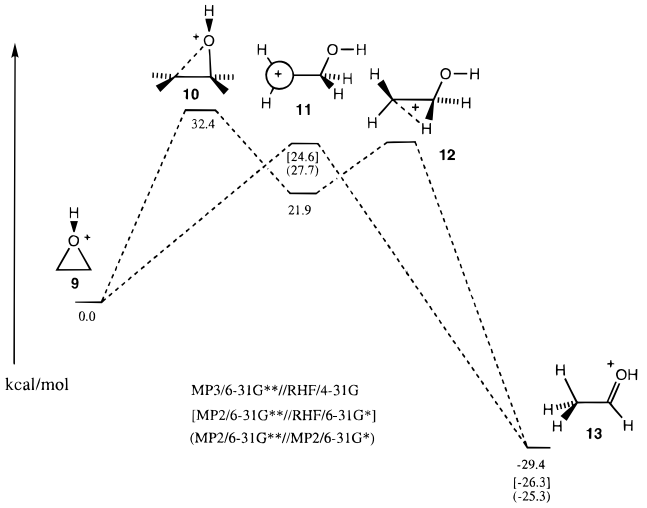

Figure 2. Acid-catalyzed rearrangement of oxirane.

Ab initio calculations of the acid-catalyzed rearrangement of ethylene oxide to acetaldehyde in the gas phase show protonated epoxide **9** to be an energy minima on the potential energy surface.[7] These early studies of the $C_2H_5O^+$ potential energy surface at the MP3/6-31G**//RHF/4-31G level[8] suggested carbocation **11** to be an intermediate to protonated acetaldehyde **13**. A transition structure **10** between **9** and **11** was identified along with a small activation barrier from **11** to a transition structure for rearrangement to **13**. With the inclusion of polarization functions in the basis set and incorporation of electron correlation the energy of **12** falls below that of the intermediate **11**. Thus although cation **11** is predicted to be stable with respect to cyclization to **9** and with respect to a 1,2-proton shift to protonated vinyl alcohol Radom et al.[7] suggested it was unlikely to be an observable species because of facile rearrangement by means of a 1,2-hydride shift to **13**.

Later calculations at the MP2/6-31G**//HF/6-31G*[9] and MP2/6-31G**//MP2/6-31G*[10] levels predict gas-phase unimolecular ring opening of protonated oxirane **9** to lead to protonated acetaldehyde **13** via an activation barrier of 24.6 and 27.7 kcal/mol, respectively, with no intervening minima. A transition structure **11** was established with the C2 cation p orbital orthogonal to the C2−C1−0 plane. The imaginary vibration exhibited a twist of the hydrogens on C2 and rotation of a hydrogen on C1 into the plane of the p orbital of the cation.[8]

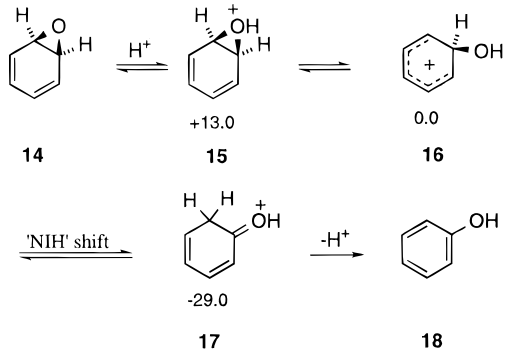

Figure 3. Arene oxide rearrangement.

The migrating hydrogens of **9** in the rearrangement to **13** are diastereotopic with respect to the proton on oxygen. However, the symmetry of the cation **11** precludes differentiation in hydrogens in the migration. In contrast, rearrangement of protonated fluorooxirane was calculated (MP2/6-31G*//MP2/6-31G*)[9] to open to protonated aldehyde by two stereospecific pathways involving carbocation intermediates.

In contrast to the calculations for acid-catalyzed rearrangement of ethylene oxide, acid-catalyzed opening of benzene oxide, styrene oxide, and analogous substituted epoxides in the gas phase are calculated by *ab initio* methods to give carbocations as energy minima.[11] The rearrangement of these epoxides is therefore considered stepwise. For the rearrangement of benzene oxide (**14**) to phenol (**18**), calculations[12] at the MP2/6-31G*//RHF/6-31G* level of theory show the hydroxycyclohexadienyl cation **16** to be an intermediate 13 kcal/mol lower in energy than the protonated oxirane **15**. The protonated dienone **17** resulting from ring opening of **15** followed by a NIH shift is calculated to be 42 kcal/mol lower in energy than **15**. The oxonium ion **15** was considered to be the transition state for the interconversion of the two otherwise identical carbocation structures in which the HO group is located at adjacent carbons. Carbocation **16** could collapse to phenol by proton loss from C1 or undergo a NIH shift, the latter being favored (Figure 3). From studies of deuterium-labeled substrates, it was shown that the NIH pathway is energetically favored.

Carbocations rather than oxonium ions have been similarly calculated to be intermediates in the rearrangement of monohydroxy, amino, and vinyl oxiranes at the RHF/6-31G*//RHF/6-31G* level of theory.[10] For oxirane and the fluoro, methyl, cyano, formyl, and formaldimino derivatives, both *anti* and the *syn* oxonium ions, which differ in energy by less than 2 kcal/

(7) Nobes, R. H.; Rodwell, W. R.; Bouma, W. J.; Radom, L. *J. Am. Chem. Soc.* **1981**, *103*, 1913.
(8) The MP3 results are estimated.[7]
(9) Ford, G. P.; Smith, C. T. *J. Am. Chem. Soc.* **1987**, *109*, 1325.
(10) Bock, C. W.; George, P.; Glusker, J. P. *J. Org. Chem.* **1993**, *58*, 5816.
(11) George, P.; Bock, C. W.; Glusker, J. P. *J. Phys. Chem.* **1992**, *96* 7302.
(12) George, P.; Bock, C. W.; Glusker, J. P. *J. Phys. Chem.* **1990**, *94*, 8161.

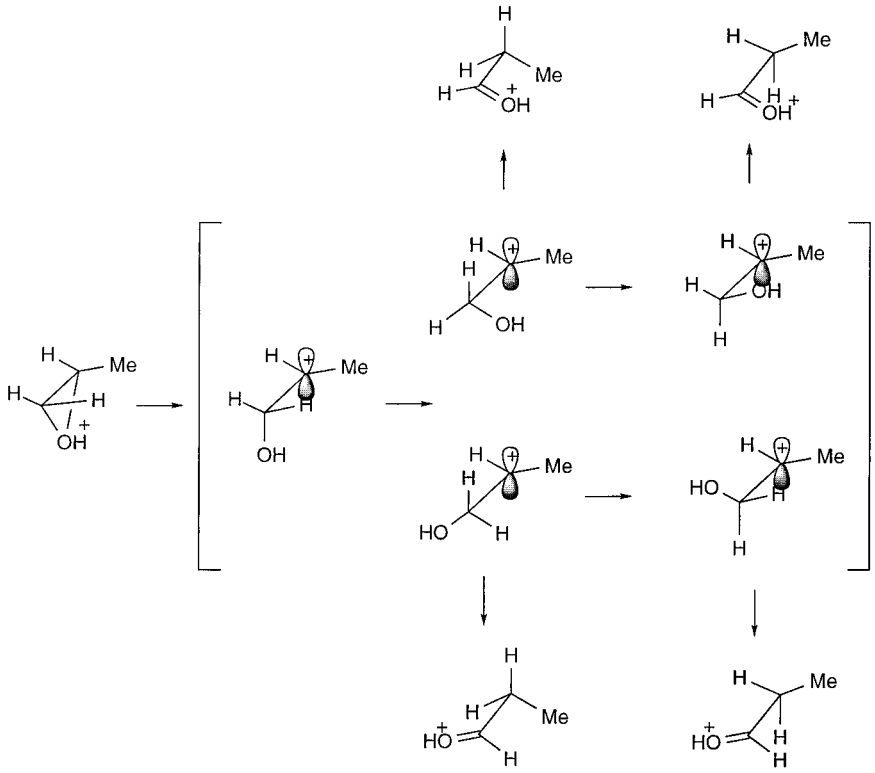

Figure 4. Schematic representation of acid-catalyzed rearrangement of propene oxide.

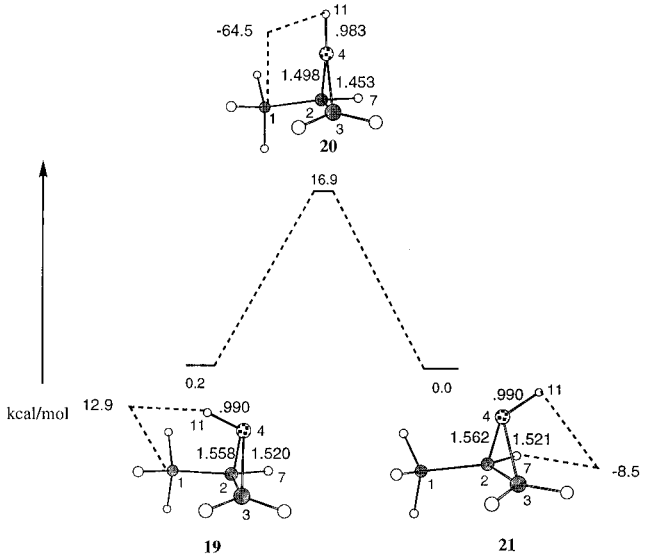

Figure 5. Intramolecular interconversion of stereoisomeric protonated propene oxides. (Dashed lines refer to dihedral angles C1−C2−O4−H11 for **19** and **20** and H7−C2−O4−H11 for **21.**)

mol, are calculated to be more stable than the corresponding carbocations. In previous work, *syn* and *anti* oxonium ions have been referred to as invertomers.[10] The corresponding carbocations are intermediates but are consistently higher in energy than the protonated epoxides.

We now report calculations on the proton catalyzed rearrangement of propene oxide in order to define in detail the potential energy surface for the more important regions of the rearrangement process.

Computational Methods

Exploratory calculations were carried out at semiempirical (AM1**)** and Hartree−Fock (3-21G, 6-31G*) levels. All results reported here, including optimized structures, vibrational frequencies, and intrinsic reaction coordinate (IRC) paths, were derived from MP2/6-31G* calculations using the GAUSSIAN 94[13] suite of programs. Correlation corrections to the level of G2(MP2) are being carried out on selected stationary points of the potential energy surface.

Results and Discussion

The acid-catalyzed rearrangement of propene oxide to propanal requires ring opening and hydrogen migration (Figure 4). The extent to which the hydrogen is aligned with the developing carbocation center for migration is a matter for investigation and related to the nature of the potential energy surface defining a concerted synchronous, concerted asynchronous or stepwise rearrangement. This investigation addresses this question and the location and importance of the structures enclosed in brackets in the simplified scheme (Figure 4) on the potential energy surface are assessed by *ab initio* calculations.

Protonation of propene oxide can occur on either face of the oxirane ring to give the stereoisomeric *syn* and *anti* oxonium ions **19** and **21**. At all levels of theory the *syn* coordinated oxonium ion **19** was found to be marginally higher in energy than the *anti* oxonium ion **21**, at the MP2/6-31G* level of theory by 0.2 kcal/mol.[14] Protonation of propene oxide is expected to be reversible and the diastereomers most likely interconvert in this way. However, an intramolecular transition structure **20** has been established 16.9 kcal/mol higher in energy than **21**.

(13) Frisch, M. J.; Trucks, G. W.; Schlegel, H. B.; Gill, P. M. W.; Johnson, B. G.; Robb, M. A.; Cheeseman, J. R.; Keith, T.; Petersson, G. A.; Montgomery, J. A.; Raghavachari, K.; Al-Laham, M. A.; Zakrzewski, V. G.; Ortiz, J. V.; Foresman, J. B.; Cioslowski, J.; Stefanov, B. B.; Nanayakkara, A.; Challacombe, M.; Peng, C. Y.; Ayala, P. Y.; Chen, W.; Wong, M. W.; Andres, J. L.; Replogle, E. S.; Gomperts, R.; Martin, R. L.; Fox, D. J.; Binkley, J. S.; Defrees, D. J.; Baker, J.; Stewart, J. P.; Head-Gordon, M.; Gonzalez, C.; Pople, J. A. *Gaussian 94, Revision B.1*; Gaussian, Inc., Pittsburgh PA, 1995.

(14) Similar results have been noted by George[10,11] who reported that the inclusion of electron correlation at the MP2/6-31G*//RHF/6-31G* level does not change these small energy differences to any appreciable extent.

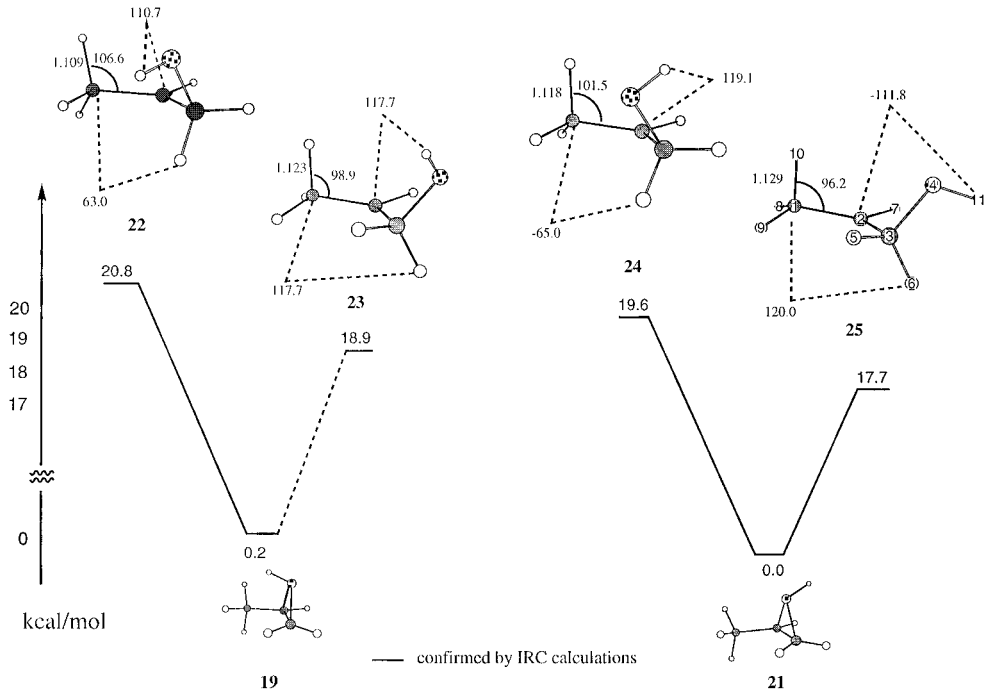

Figure 6. Transition structures involved in the potential energy surface for ring cleavage of protonated propene oxide. (Dashed lines refer to dihedral angles C1−C2−C3−H5 and C2−C3−O4−H11 for **22** and **24** and C1−C2−C3−H6 and C2−C3−O4−H11 for **23** and **25**.)

Four transition structures involving ring cleavage of **19** and **21** have been established, each involving rupture of the more substituted C−O oxirane bond and rotation about the C^+−CH_2−O bond. The energies of these transition structures are within 3 kcal/mol. Importantly the calculations quantify the preference for oxygen to rotate away from the methyl and relieve the skew oxabutane interaction. Such rotation is favored by *ca.* 2 kcal/mol (Figure 6).[15]

Three features of the structures are of particular note. The first is the importance at the transition structure of CH hyperconjugation from the methyl hydrogen in the plane of the carbocation p orbital. This CH is bent toward the carbocation and the H10−C1−C2 angle in **25** is 96°. Furthermore the CH bond is extended in length (1.129 Å). Similar but less marked effects are observed in the other three higher energy transition structures. The second feature of note is that at the transition structures the optimized bond angles (C2−C3−H6 angles are 109−110° and the C1−C2−C3 angles 122−126°, respectively) suggest that C2 and C3 are essentially sp^2 and sp^3 hybridized.[16] Finally of note is that C3**H**6 has not started to migrate at the transition structures nor is the C3−H6 bond aligned with the carbocation p orbital, the C1−C2−C3−H6 dihedral angles being some 25−30° from the plane of the carbocation p orbital.

In view of the large structural differences between transition structures, reactants and products, IRC paths were determined to establish connectivities. The most favored pathway for ring cleavage involves transition state **25**. It seemed pertinent to study this pathway in some detail. An intrinsic reaction coordinate calculation (IRC) was performed at the MP2/6-31G* level and showed the transition structure to collapse to protonated epoxide **21** and protonated aldehyde in conformation **26** (Figure 7).

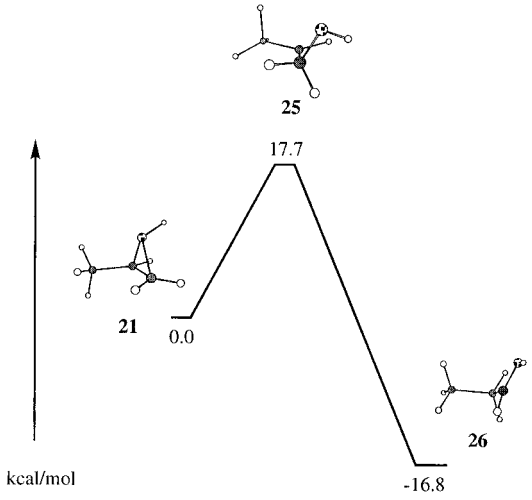

Figure 7. Intrinsic reaction coordinate relating **21** and **26**.

A movie file, available as Supporting Information,[17] graphically shows the discrete stages of the reaction. Analysis of the reaction trajectory reveals two major distinct and interdependent processes: first, rupture of the oxirane and second, hydride migration. The overall reaction profile via this transition structure is consistent with an asynchronous concerted rearrangement elaborated in some detail below.

The variation of the C1−H10 bond length, H10−C1−C2 bond angle, and the H10−C1−C2−C3 torsional angle with reaction coordinate are shown in Figure 8. In the very early stages of reaction, before any other changes are observed, the methyl begins to rotate to bring the C1−H10 bond into alignment with the developing carbocation center at C2 as shown by the variation in the torsional angle H10−C1−C2−C3 with reaction coordinate. This dihedral angle reaches a minimum of 96° at the transition structure. The importance of hyperconjugation by a methyl hydrogen in stabilizing the transition structure is shown by the H10−C1 bond length which is longest

(15) The energy difference is greater than between **19** and **21** which reflects the hydrogen atom configuration in the two diastereomers.

(16) However the size of the C2−C3−H6 and C1−C2−C3 angles may very well be an artifact of the difference in mass and vdw between H and C.

(17) See Supporting Information.

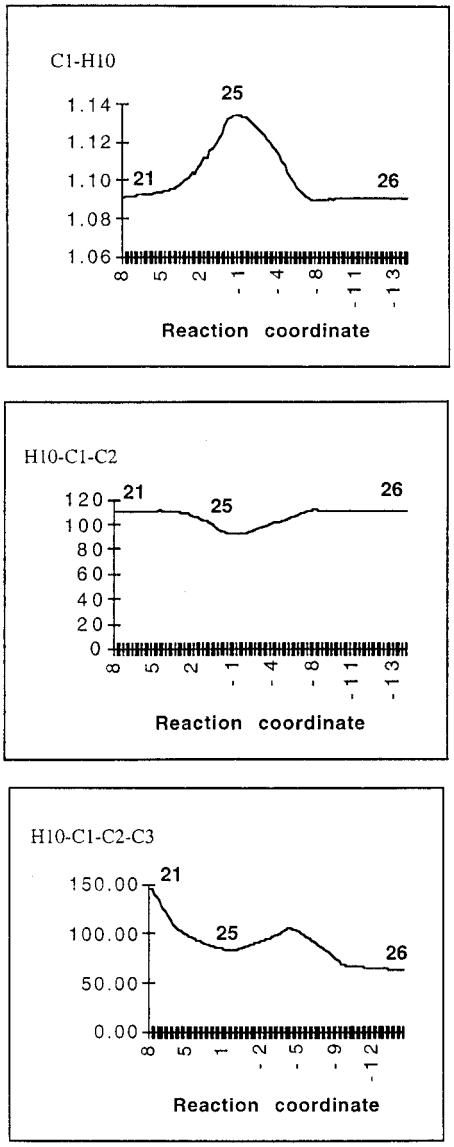

Figure 8. The importance of hyperconjugation.

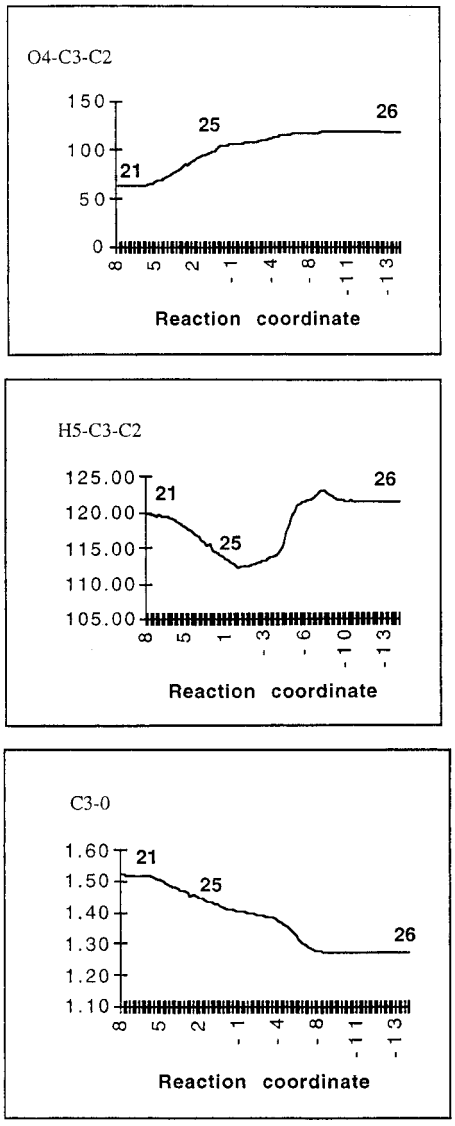

Figure 9. Oxirane ring rupture.

and the H10−C1−C2 bond angle which is most compressed at the transition structure. The demand for hyperconjugation at the transition structure is consistent with the charge development at C2 being greatest at this point in the reaction coordinate.

At the transition structure the oxirane ring has opened such that C2 and C3 are essentially sp^2 and sp^3 hybridized respectively according to the optimized C2−C3−H6 and C1−C2−C3 bond angles. With rupture of the epoxide the O−C3−C2 angle increases so that at the transition structure this angle is 102°, just short of tetrahedral, and thereafter increases to that for sp^2 hybridization as in protonated aldehyde (Figure 9). Concomitant with C2−O bond rupture is rehybridization at C3 to tetrahedral. A notable feature apparent in the plot of C3−O bond distance with reaction coordinate is that the double-bond character of the protonated carbonyl is formed late in the reaction coordinate, in a second step of the reaction profile.

The migration of hydride is late in the reaction coordinate with the C3−H6 distance remaining constant well past the stage where the oxirane ring has ruptured. The transfer of hydride coincides with a change in the hybridization at C2 from sp^2 to sp^3, which is reflected by the C3−C2−C1 and H6−C3−C2 angles (Figure 10).

Two other stationary points **28** and **29** were established on the reaction surface (Figure 11). For both these structures C1−C2−C3−OH are planar. Structure **29** is flanked by minima where the eclipsing of the C−O with the adjacent CH is relieved by a change in the torsional angle of 2°. Surprisingly **29** is computed at the MP2/6-31G* level to be higher in energy than **28** where the oxygen is *cis* to the methyl. An IRC calculation shows the connection of **19** via transition state **22** to **28**. A surface between **28** and aldehyde has not been established. The importance of **29** on the reaction surface was also difficult to elaborate but the structure optimized to **26**, shown by a dotted line in Figure 11.

An IRC calculation of transition structure **24** shows it to be linked to aldehyde **27** and protonated epoxide **21**. The calculation failed before reaching the aldehyde and protonated epoxide but had progressed sufficiently in each direction to establish this concerted asynchronous pathway between **21** and **27**. The broken lines represent extrapolations based on the last geometry reached. At each of the break points in Figure 11, the IRC algorithm suddenly failed to optimize to the IRC path and terminated abruptly with a bizarre extrapolation of the geometry. We speculate that the failure may be due to a bifurcation point, *i.e.*, a point where a zero force constant for a normal mode perpendicular to the IRC is encountered. Conformation **27** of the protonated aldehyde is computed to be 0.5 kcal/mol lower in energy that conformation **26**, consistent with the known

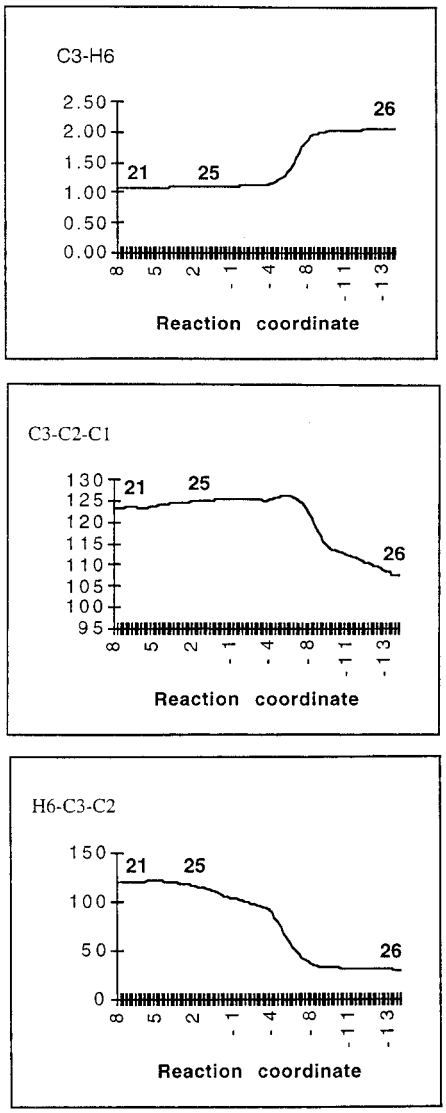

Figure 10. Hydride migration.

preference of a carbonyl to eclipse with a C−C bond in preference to a C−H bond.

An IRC calculation for transition structure **23** showed it going to **26** but the surface on the other side of the transition structure was difficult to define because methyl rotation resulted in a minimum close to transition state **23** despite the fact that atomic trajectories of **23** along the normal mode with imaginary frequency gave no evidence for this motion.

The lowest energy concerted reaction coordinate diagram connecting **21** and **26** via transition structure **25** summaries an asynchronous but concerted reaction surface for the acid-catalyzed rearrangement of propene oxide (Figure 12).

The reaction surface is characterised by (i) methyl rotation and ring opening which leads directly to the transition structure **25**, (ii) preparation for hydride transfer stage (*i.e.* the plateau), (iii) hydride transfer itself at the rapid drop from the plateau, (iv) a flat approach to a low energy conformation of protonated aldehyde.

Unlike a tertiary epoxide (Figure 1) the calculations show a potential energy surface for rearrangement of protonated propene oxide which does not require a discrete carbocation intermediate. Any diastereoselectivity in the rearrangement will reflect the relative preference for the transition structures **25** and **23** versus **24** and **22** (Figure 6). The calculations, using a Boltzmann distribution, predict a 20:1 preference for migration of the proton *trans* to the methyl over the *cis*.

Conclusion

High level *ab initio* calculations show that concerted asynchronous pathways exist between protonated propene oxide and protonated propanal. The preferred pathway connects **21** via **25** to **26** (Figures 7 and 12). In the cleavage of the C−O bond the preference for rotation of oxygen away from the more hindered face of the oxirane plane containing the methyl is quantified as 2 kcal/mol. The reaction is predicted to show a 20:1 preference for migration of the proton *trans* to the methyl over the *cis*, The lowest energy pathway involves two distinct steps. The first step, rupture of the oxirane ring, is followed by a

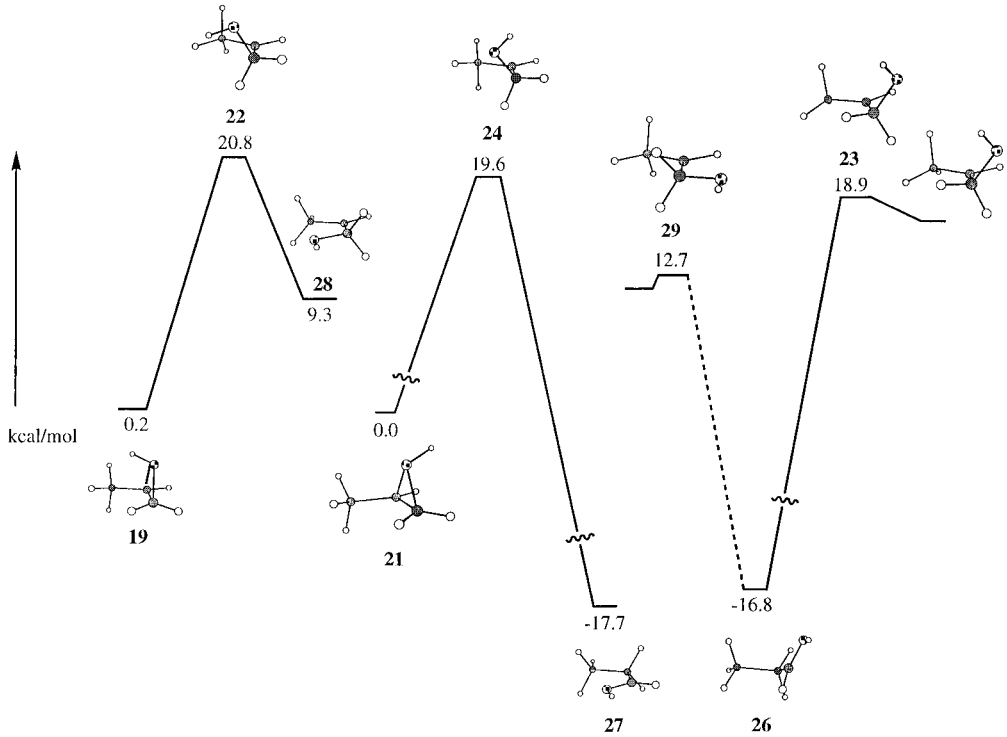

Figure 11. Reaction surface connecting protonated propene oxides and aldehydes.

Table 1. MP2/6-31G*//MP2/6-31G* calculations[a]

structure	energy (au)	ZPC (au)	energy − ZPC (kcal/mol)	imag freq	$E - E(21)$ (kcal/mol)
19	−192.804 61	0.100 50	−120 926.909 5		0.2
21	−192.804 86	0.100 45	−120 927.098 0		0.0
28	−192.784 74	0.094 91	−120 917.777 3		9.3
26	−192.831 39	0.100 14	−120 943.926 1		−16.8
27	−192.832 31	0.099 63	−120 944.811 1		−17.7
TS					
20	−192.775 76	0.098 07	−120 910.253 1	971	16.8
22	−192.767 58	0.096 07	−120 906.317 2	380	20.8
23	−192.770 00	0.095 41	−120 908.227 9	240	18.9
24	−192.768 94	0.095 52	−120 907.494 2	346	19.6
25	−192.772 09	0.095 63	−120 909.405 7	202	17.7
29	−192.779 04	0.094 60	−120 914.378 1	96	12.7

[a] (ZPC scaled by 0.95).

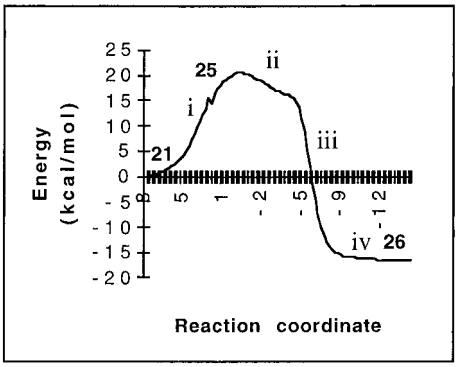

Figure 12. Lowest energy reaction coordinate diagram connecting **21** and **26** via transition structure **25**: (i) ring opening, (ii) preparation for hydride transfer, (iii) hydride transfer, (vi) approach to a low-energy conformation of protonated aldehyde.

second step, hydride migration, a process not commenced until breaking of the C−O bond is complete. The combination of these two steps defines a concerted asynchronous pathway. Of special interest is the fact that carbocation **28** with the methyl and hydroxy groups *cis* is calculated to be 3 kcal/mol more stable than the corresponding *trans* isomer. Yet rearrangement of the protonated propene oxide to protonated propanal by ring opening in the direction of the less stable *trans* carbocation is calculated to be the favored pathway for isomerization.

Acknowledgment. J.M.C. acknowledges a Visiting Killam Scholarship of the University of Calgary. We (J.M.C. and D.W.) acknowledge a NSF(US)-NZ Joint collaborative research award funded by NSF(US) and MOST(NZ). We acknowledge grants from the New Zealand Lotteries Board.

Supporting Information Available: Archive material on all stationary points (29 pages) and the movie file mentioned in Results and Discussion (electronic form only). See any current masthead page for ordering and Internet access instructions.

JA963057N